Available online at www.sciencedirect.com
ScienceDirect
Polymer 48 (2007) 5069–5079
polymer
www.elsevier.com/locate/polymer

The development of microstructure in oriented polyethylene terephthalate (PET) during annealing

Ahmed I Abou-Kandil*, Alan H Windle

Department of Materials Science and Metallurgy, University of Cambridge, Pembroke Street, Cambridge CB2 3QZ, UK

Received 4 April 2007; received in revised form 10 May 2007; accepted 19 June 2007
Available online 24 June 2007

Abstract

This work concerns the changes in structural order, which occur when amorphous polyethylene terephthalate (PET) is crystallised by drawing and then subsequent annealing. Real time wide angle X-ray fibre diffraction is used to obtain information about the microstructural changes taking place during drawing and subsequent annealing. The diffraction patterns obtained proved the existence of a liquid crystalline transient mesophase prior to crystallisation. The development of both the mesophase and the crystalline structure are also studied using small angle X-ray scattering during annealing of uniaxially drawn samples held at constant strain. These experiments proved the absence of any microstructure associated with the mesophase and that significant microstructural changes take place only when crystallisation starts to occur.

Keywords: Polyethylene terephthalate; WAXS; SAXS

1. Introduction

Uniaxially deformed fibres and films of PET produced under normal processing conditions contain three-dimensional ordered crystalline phase in which the polymer chain axis is closely aligned with the principal deformation axis. Bonart [1,2] was the first to report the occurrence of paracrystalline structure. He observed that the structure of PET varied during the drawing treatment from a totally amorphous to a nematic and finally a smectic state. Comparatively recently, Keller underlined the thermodynamic grounds for mesophases being favoured in an intermediate step in the crystallisation of polymers [3]. In unoriented PET, Imai et al. [4] have presented evidence from SAXS that density fluctuations develop via a spinodal process. They interpreted these as being precursors to the crystal nucleation process. In a series of papers Welsh et al. [5,6] announced the observation of a liquid crystalline transient smectic mesophase in drawn quenched samples and during drawing of PET, PEN and their copolymers. Asano et al. [7,8] reported that during annealing of oriented amorphous PET an initial nematic type order is transformed into a smectic order before triclinic crystals are formed. Mahendrasigam et al. [9,10] studied the effect of draw ratio on strain induced crystallisation of PET at fast draw rates and have also recently reported diffraction evidence of mesophase diffraction in PET while being rapidly deformed. Blundell et al. [11] described the development and decay of the mesophase during drawing of the 50% PET/PEN copolymer. Jackeways et al. [12] and Carr et al. [13] also reported the presence of the mesophase in PEN fibres. Also some authors attempted to model the structure of the PET mesophase. Auriemma et al. [14,15] through a series of experimental and modelling studies, concluded that a model of isolated chains could qualitatively account for the observed mesophase pattern with monomer units in random minimum energy conformations. Nicholson et al. [16] found that the energy minima for the

* Corresponding author. Present address: Max-Planck Institute for Polymer Research. Ackermannweg 10. Mainz. Germany. 55128.
E-mail address: camaia23@yahoo.co.uk (A.I. Abou-Kandil).

0032-3861/$ - see front matter © 2007 Elsevier Ltd. All rights reserved.
doi:10.1016/j.polymer.2007.06.042

CO–O–C–C dihedral angles in PET are close to 80°. They also suggested that there are two stable conformations of PET and that one of them might be responsible for the appearance of the mesophase reflection.

In the study by Welsh et al. [5,6] WAXS and SAXS diffraction patterns were reported for a series of crystalline PET/PEN random copolymers. However, in all the previous reports no detailed SAXS/WAXS studies have been performed to account for the presence of microstructure associated with the appearance of the mesophase. A series of WAXS and SAXS experiments performed under exactly the same conditions will be used to shed more light on the development of microstructure during annealing of oriented PET samples.

2. Experimental

2.1. Sample preparation

Amorphous PET films of 500 μm initial thickness were used. The intrinsic viscosity of PET was 0.9, as given by the supplier, ICI. The molecular weight of the polymer was found to be about 82,000 g/mol, which was calculated using Kuhn–Mark–Houwink equation [17]:

$$[\eta] = \kappa M_v^{\alpha} \tag{1}$$

The constants for PET are $\alpha = 0.695$ and $\kappa = 5.2 \times 10^{-4}$ ml/g [18].

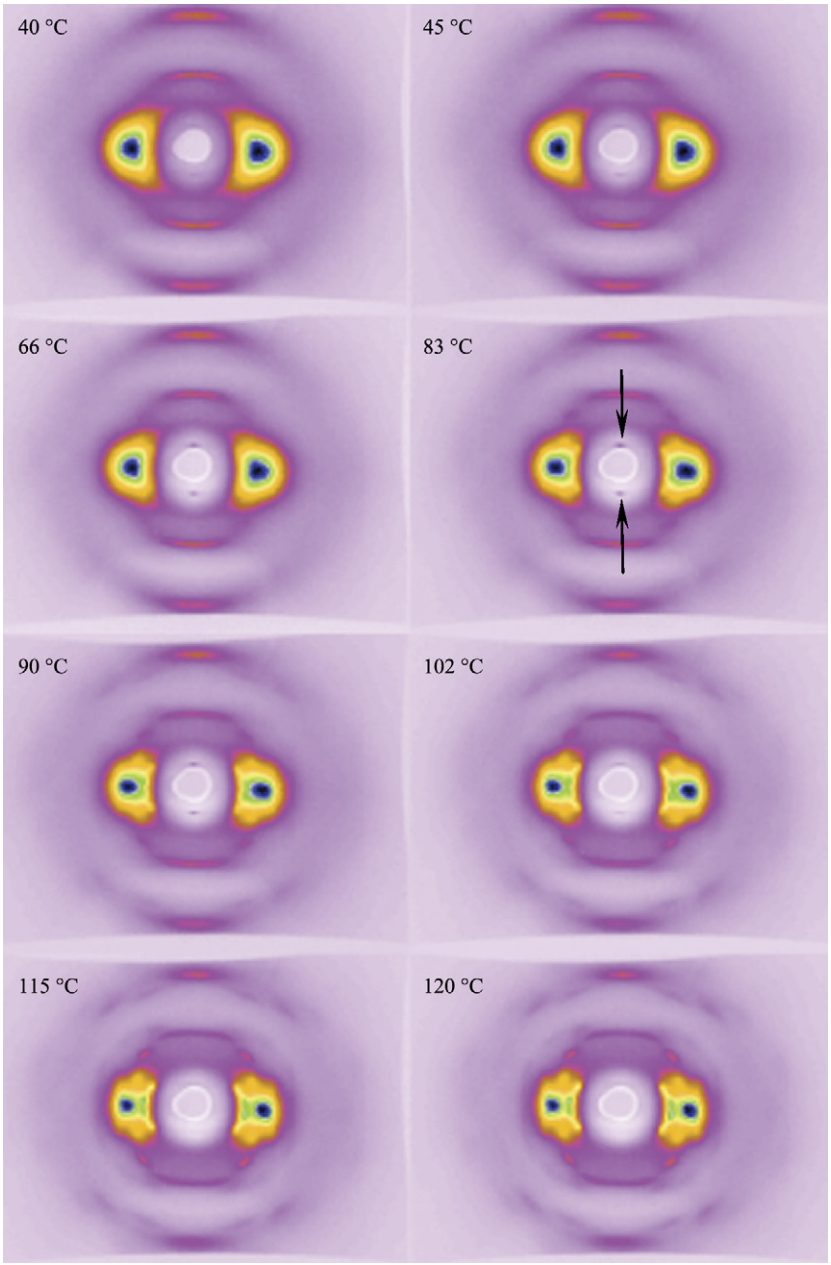

Fig. 1. X-ray fibre diffraction patterns of PET taken at different temperatures, as indicated in the figure. The sample was drawn at 40 °C to a draw ratio of approximately 3.5 and at a draw rate of about 0.037 mm s^{-1}. It was continuously heated to 90 °C, held at 90 °C for approximately 8 min and then continuously heated again to 120 °C. The arrows indicate the mesophase reflection at its maximum intensity at 83 °C.

2.2. WAXS and SAXS analysis

The WAXS diffraction experiments were performed at the European Synchrotron Radiation Facility (ESRF), Grenoble, France, using beam line ID1 (wavelength of the X-ray beam is 1 Å). The SAXS experiments were performed in the synchrotron radiation source (SRS), Daresbury, UK using beam line 16.1 (wavelength of the X-ray beam is 1.41 Å). Detailed information on both beam lines can be found in www.esrf.fr and www.srs.ac.uk, respectively. The experiments used a purpose-designed X-ray diffraction camera constructed at the University of Keele [19].

Rectangular samples, 10 mm wide, were clamped inside the camera at 40 °C and drawn at approximately 0.037 mm/min to a draw ratio of 3.6. The sample was then heated gradually to 130 °C. The WAXS diffraction patterns were obtained during the heating process. A single frame of resolution 768 × 576 pixels was taken using a Photonics Science CCD detector, with a sensitive area 92 mm × 69 mm and effective pixel area of 120 μm × 120 μm. The sample to detector distance was as small as 6 cm. At this sample to detector distance, a *d*-spacing between ~15 Å and ~1.5 Å can be recorded. Each diffraction pattern was recorded with an exposure time of 10 s once the sample reached the set point. After each diffraction pattern has been taken the sample was left to equilibrate at this temperature for 120 s, then another diffraction pattern was recorded. The sample to detector distance was calibrated using silicon powder that gives a sharp 100 ring at a *d*-value of 3.135 Å.

SAXS diffraction patterns were obtained using a rapid detector at a resolution of 512 × 512 pixels. Each SAXS frame was collected for 180 s. A sample to detector distance of about 3.5 m was used, allowing a q range from 0.093 nm^{-1} to 1.16 nm^{-1} (674–54 Å) to be accessed. The data was calibrated using wet rat tail collagen.

Data was corrected for air scatter by subtracting an empty camera data file, taken under the same conditions, from the experimental data. A simple manual method was used to determine the local draw ratio, which was done by measuring the separation of marker lines on either side of the point on the sample on which the X-ray beam impinges. Manual measurements of the draw ratio for each data frame were taken from a video camera, which also serves as a record of the general behaviour of the sample during the draw.

3. Results

3.1. WAXS

Amorphous PET samples were drawn at approximately 0.037 mm/s to a draw ratio of 3.6 at 40 °C. The sample was then removed from the tensile machine and divided into two parts vertically in the direction of the draw. One strand was then returned to the tensile machine and re-clamped under stress. It was then gradually heated from room temperature to 90 °C, held at this temperature for approximately 8 min and then heated to 130 °C. One WAXS diffraction pattern was taken every 5 °C for 10 s.

Fig. 1 shows the two-dimensional diffraction patterns of PET sample drawn at 40 °C. It is clear that uniaxially drawing the sample at this temperature leads to the formation of an oriented amorphous structure. The main equatorial feature of the pattern at this temperature is a diffuse peak within the amorphous halo at about 4.17 Å. The pattern also shows a sharp meridional reflection at 10.42 Å and broader high angle meridional reflections at 5.57 Å, 3.54 Å and 2.08 Å. By increasing the temperature gradually the intensity of the low angle meridional reflection, mesophase reflection, increases gradually till it reaches a maximum intensity at 83 °C. At this temperature the equatorial reflections are still diffuse and do not show any signs of splitting due to crystallinity. When the temperature reaches 90 °C the intensity of the low angle meridional reflection starts to decrease while the equatorial reflections start to split indicating that the sample is starting to crystallise. The gradual increase of temperature leads to the gradual decrease in the intensity of the mesophase reflection and the formation of well-defined sharp equatorial peaks. This can be seen more clearly in Fig. 2, which shows meridional and equatorial scans taken at each temperature as shown in Fig. 1.

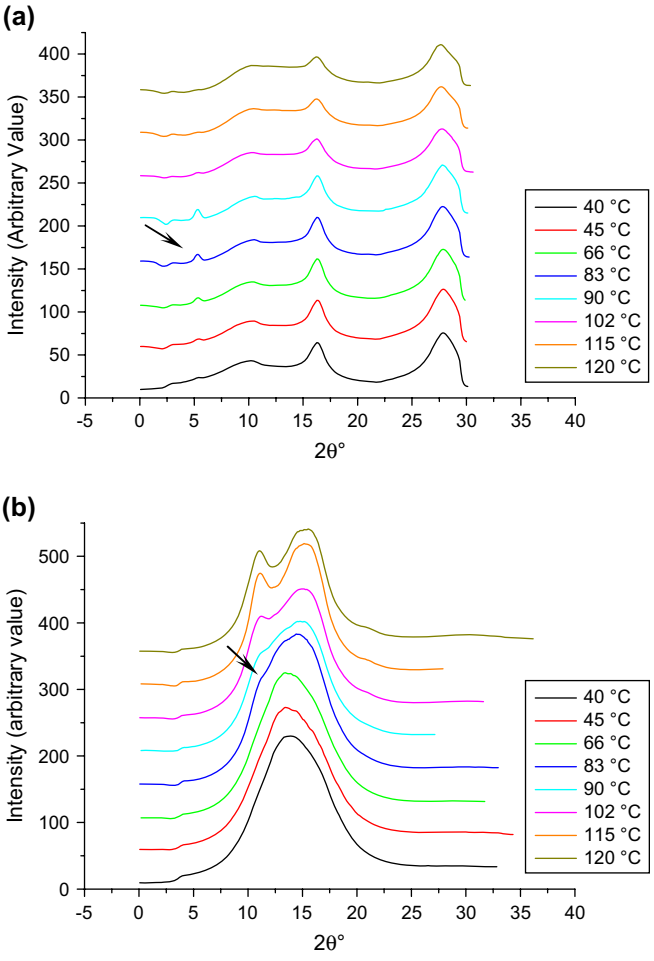

Fig. 2. (a) Meridional and (b) equatorial scans of the two dimensinal diffraction patterns shown in Fig. 1, showing the mesophase development and the onset of crystallinity at 83 °C. The arrow in figure (a) points at the maximum mesophase intensity and in figure (b) shows the first beginning of crystallisation.

The sample was held at 90 °C for about 8 min; during that time a diffraction pattern was taken every minute. It is clear from Figs. 3 and 4 that holding the sample at this temperature also leads to a gradual decrease in intensity of the mesophase reflection with the development of the crystalline equatorial peaks. The amount of the mesophase and crystalline component are actually related to the integrated area under the reflection, but because the Gaussian half-width of the reflections underwent very little change during the course of the experiment, a semi-quantitative study can be completed by simply considering the peak intensities. This approach has also been proved successful in previous studies on PET [20].

Fig. 5 shows the development of the mesophase meridional reflection and the 010 reflection (as an estimate of crystallinity) intensities as a function of both temperature and time. It is clear from Fig. 5a that the amount of the intensity of the mesophase reflection reaches maximum at 83 °C, after this temperature intensity decreases again and crystalline peaks start to appear. It is also clear from Fig. 5b that at 90 °C the crystallinity increases with time while the mesophase shows an opposite behaviour.

The increase of order with the development of the intermediate smectic-A structure prior to the formation of the triclinic crystals has also been monitored by measuring P_2 as described by Lovell and Mitchel [21]. Azimuthal scans were taken at approximately 3.54 Å, which corresponds to a maximum in the equatorial scan [10,11]. The development of P_2 with respect to temperature and time is shown in Fig. 6. Fig. 6a clearly shows the increase in the value of P_2 with temperature, reaching a maximum at 66 °C and then it starts to decrease gradually from 83 °C until 120 °C.

On the other hand when P_2 is monitored as a function of time as the sample is annealed at constant temperature as shown in Fig. 6b it is clear that the value of the orientation parameter is nearly constant and does not change with time. It only decreases slightly with prolonged annealing at that temperature. The behaviour of P_2 with temperature and time is discussed in more detail below. The percentage crystallinity attained at the end of this experiment has been measured as described by Blundell [22], and was found to be 28.6%.

3.2. SAXS

A rectangular PET sample having an intrinsic viscosity (IV) of 0.9 was drawn as explained above. The sample was kept under constant strain with its ends fixed to prevent

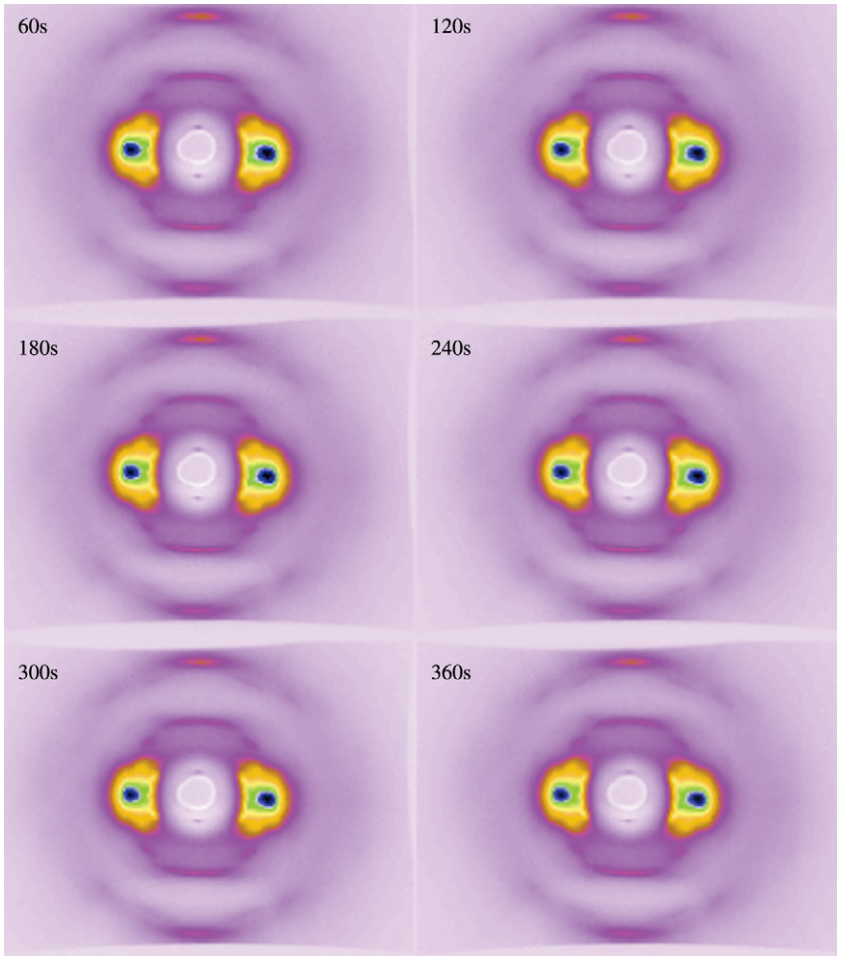

Fig. 3. X-ray fibre diffraction patterns of PET held at 90 °C for about 8 min. Diffraction patterns are taken at 60 s intervals as indicated in the figure.

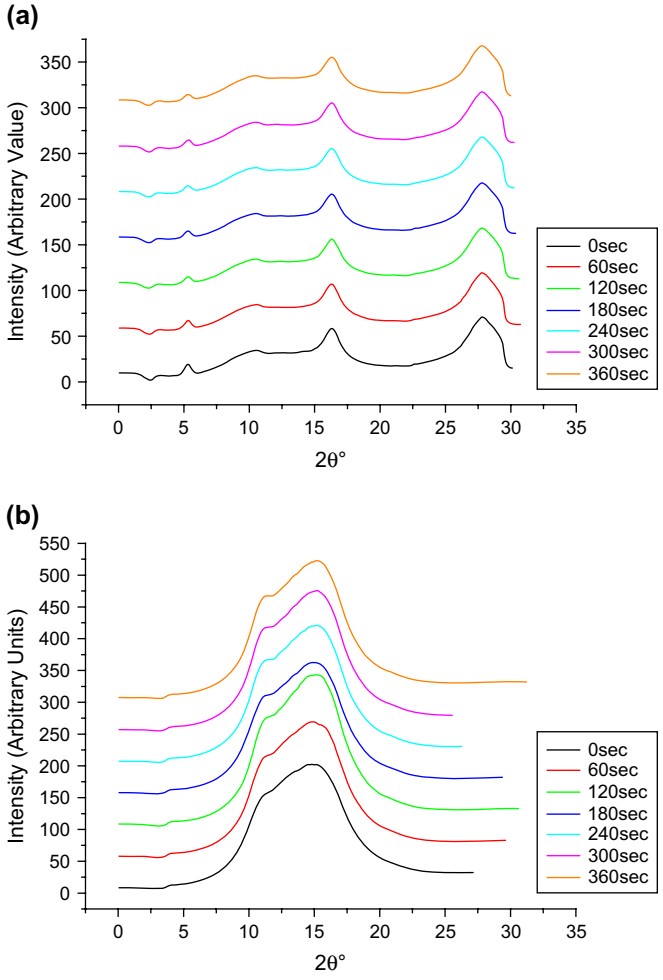

Fig. 4. (a) Meridional and (b) equatorial scans taken in the two-dimensional diffraction patterns represented in Fig. 3. This figure shows the gradual decrease in intensity of the mesophase reflection and the gradual splitting of the equatorial peaks in PET.

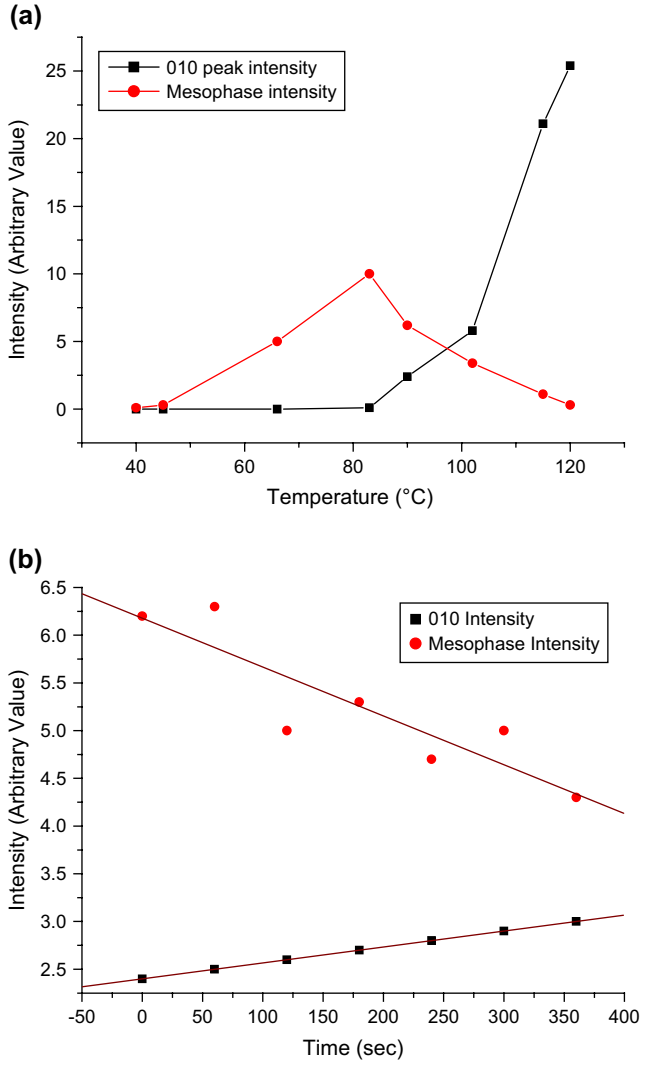

Fig. 5. (a) Represents the development of the mesophase reflection and crystallinity as a function of temperature and (b) the development of the mesophase and crystallinity as a function of time for the same PET sample kept at 90 °C for about 8 min.

thermal shrinkage and SAXS patterns were taken at different temperatures as shown in Fig. 7. It is clear from the figure that before drawing there are no significant features in these SAXS patterns, and this is an indication of the uniform electron density in the unoriented amorphous PET films. After drawing the scattering around the beam stop is changed from the circular to elliptical (oval or lemon) shape, with the minor axis of the ellipse parallel to the tensile axis. This indicates scattering from long thin structures, in this case the polymer chains, aligned approximately parallel to the draw direction. This is characteristic of small angle fibre diffraction, which has been observed earlier for PET [6] and is a well-known feature of fibre diffraction observed for various polymer systems [23,24]. The SAXS patterns remained unchanged until the temperature reached 90 °C, where a faint *four point* diffraction pattern could be observed. The intensity of the four point pattern increased gradually with increasing temperature. This indicates the gradual increase in the lateral and longitudinal packing of the crystals. This can also be observed in the WAXS diffraction patterns obtained between 80 °C and 120 °C.

When the temperature reached 110 °C the sample was kept at this temperature for about an hour to observe any changes that might take place at a temperature above the T_g of PET. At this temperature it is clear that the shape of the scattering intensity changed from a four point pattern to two broad meridional peaks forming a *two bar* pattern where some of the intensity is concentrated away from the edge of the bars, i.e. concentrated on the meridian. When the temperature reached 130 °C the two bar pattern changed to a *two point* pattern, and by increasing the temperature further the two point pattern moved towards lower q values.

The main characteristics of two-dimensional SAXS patterns were discussed in the literature [25] and specific interest was given to the interpretation of the SAXS patterns obtained for oriented crystalline PET before [8,26]. Two bar and four point patterns are characteristic of scattering from a periodic arrangement of high and low electron density regions i.e. crystalline and amorphous regions, respectively, in this case, along

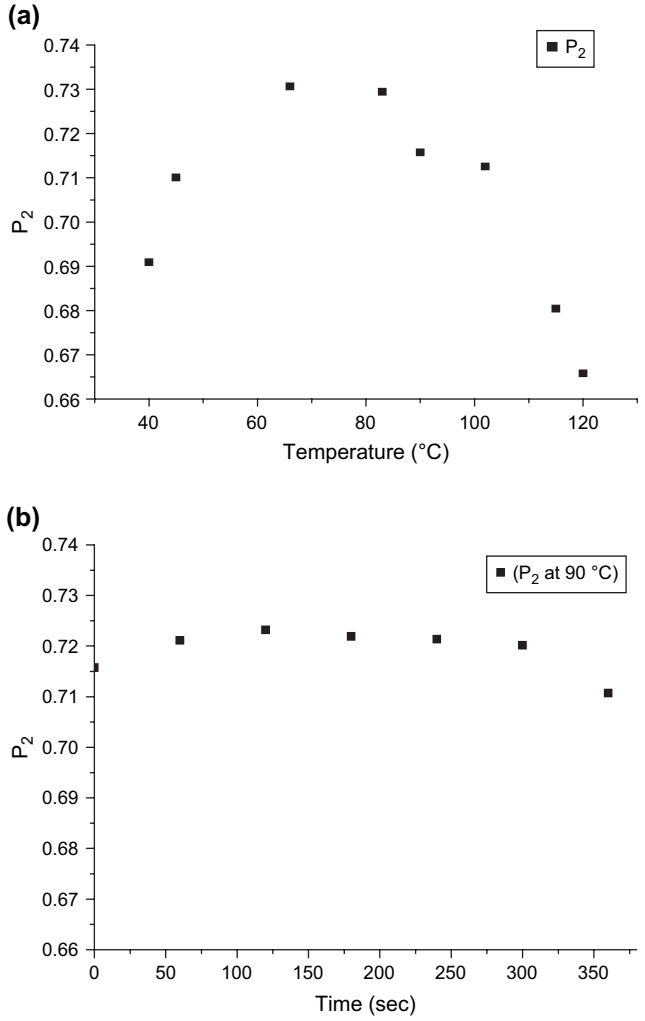

Fig. 6. (a) The development of order in PET sample as a function of temperature and (b) as a function of time for the same sample kept at 90 °C for approximately 8 min. The order is represented here by the order parameter value P_2 as explained in the text.

the length of fibrils oriented parallel to the fibre axis as shown in Fig. 8a. The lateral width of the bars varies inversely with the width of the scattering units. Four point patterns can result from a system in which amorphous and crystalline regions alternate laterally as well as axially forming a macro-lattice, Fig. 8b, or from one in which boundaries between the crystalline and the amorphous regions are sloping, Fig. 8c [27,28].

Fu et al. [29,30] investigated the possibility that four point patterns from PET fibres arise from the tilt of the *c*-axis from the fibre axis causing the crystalline surface to be inclined to the fibre direction. This idea was rejected as a much larger tilt than the two or so degrees by which PET unit cells tilt from the fibre axis would be needed to account for the observed lateral separation of the peaks in the four point patterns. Rule et al. [26] successfully modelled two bar SAXS patterns as quite disordered macro-lattices, made up of fibrils consisting of fairly periodic arrangements of crystallites, separated by amorphous regions. A frequent problem with the interpretation of SAXS is that many different possible arrangements of amorphous and crystalline material may give rise to similar SAXS patterns.

The data obtained in Fig. 7 shows that there is no significant SAXS scattering associated with the appearance of the mesophase. In the previous section it was clear that the smectic-A mesophase in PET appears at the end of the draw. These samples were drawn under the same conditions as explained here. The amount of the mesophase was seen to increase gradually with increasing temperature, reaching a maximum at 75 °C and then decreases gradually, where triclinic crystals start to appear at 80 °C. The four point pattern was only obvious at 85 °C, i.e. after crystallisation started and there was no evidence for any significant scattering at lower temperatures. This is consistent with results obtained earlier [6,8] where significant SAXS patterns were reported only for oriented annealed PET.

By integrating the two-dimensional SAXS patterns, a significant peak can only be seen at temperatures in excess of or equal to 110 °C, Fig. 9. The *long period* (LP) has been obtained at different temperatures from the SAXS patterns by measuring the distance between the peaks on either sides of the equator and applying Bragg's law to half this distance. Fig. 10 shows the variation of the long period, represented as $2\pi/\mathrm{LP}$, with temperature. The value of the LP varies significantly at different temperatures from 0.57 nm^{-1} (110 Å) at 110 °C down to 0.6 nm^{-1} (104 Å) at 150 °C and then increasing again to 0.54 nm^{-1} (115 Å) at 230 °C.

It would be inappropriate here to consider the change in the LP as a general trend because the sample was annealed at 110 °C for about an hour. This might change the arrangement or the alternation of the amorphous and crystalline regions causing the observed variation in the LP.

To judge more accurately the effect of annealing on the LP, another PET sample was drawn under exactly the same conditions. Fig. 11 shows selected two-dimensional SAXS images taken at different temperatures. Again the fibre streaking is very obvious for the sample drawn at 40 °C. A very faint four point pattern only appears at 80 °C, the intensity of the four point pattern then increases gradually with increasing temperature up to 230 °C where the four point pattern is transformed into a two bar pattern with the intensity still concentrated at the edges of the bars.

It is clear from Fig. 12 that a distinct long period does not appear except at temperatures in excess of or equal to 120 °C. The long period increases gradually with increasing temperature from 0.79 nm^{-1} (~79 Å) at 120 °C to 0.52 nm^{-1} (~121 Å) at 230 °C as shown in Fig. 13. The increase in LP with increasing temperature can be associated with the relaxation of the polymer chains that takes place at higher temperatures. This relaxation would also lead to a more ordered arrangement of the crystalline and amorphous regions with greater orientation in the direction of the draw. This might cause the change of the four point pattern to a two bar pattern at higher temperatures.

The observations made in these two experiments on PET contradict the suggestions made by Asano et al. [8], on

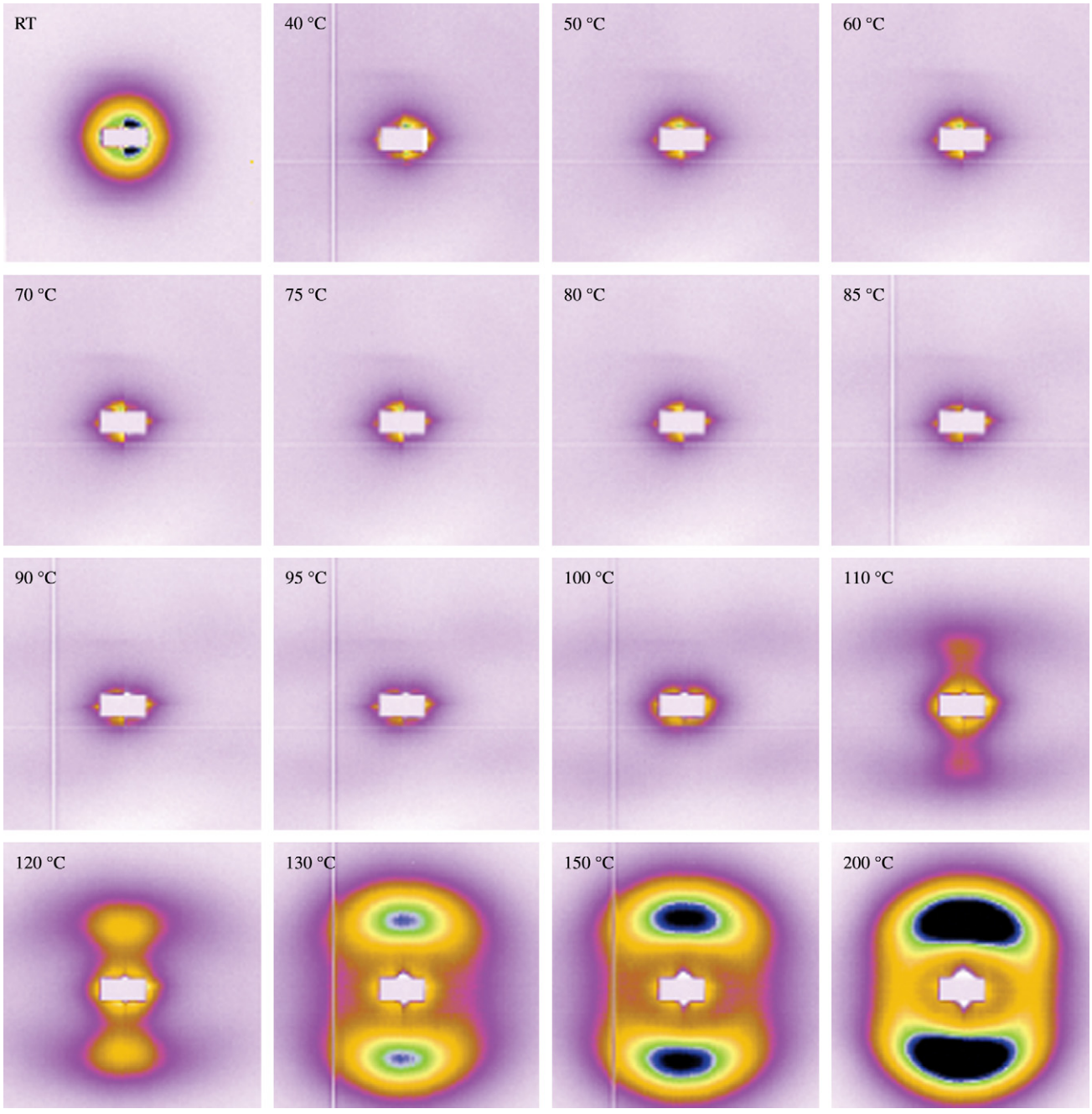

Fig. 7. Two-dimensional diffraction patterns of PET, 0.9 IV, taken at different temperatures as indicated in the figure. The sample has been drawn at room temperature to a draw ratio of approximately 3.5 and then heated gradually till 200 °C. The diffraction pattern at room temperature (RT) is undrawn and that at 40 °C is already drawn.

samples drawn under approximately the same conditions, that a two bar SAXS pattern (with maximum intensity concentrated at the centre of the bars rather than the edges) is associated with the appearance of the mesophase. However, they did not report any SAXS results that confirm this suggestion. They only reported a reflection starting to appear near the beam stop in a MAXS (middle angle X-ray scattering) experiment at 70 °C that they interpreted as the start of appearance of a layered structure prior to crystallisation. But it must be stated here that these experiments were not performed in real time and the samples were quenched drawn to a draw ratio of 3.8, annealed at each desired temperature for 10^4 s and then the diffraction pattern of each sample was collected.

However, these experiments still confirm the observation of Asano et al. [8] that the four point pattern only appears when the triclinic crystals are observed in the WAXS experiments. The results for PET, so far, show that the four point pattern is transformed into a two bar pattern and then a two point pattern which will be discussed below.

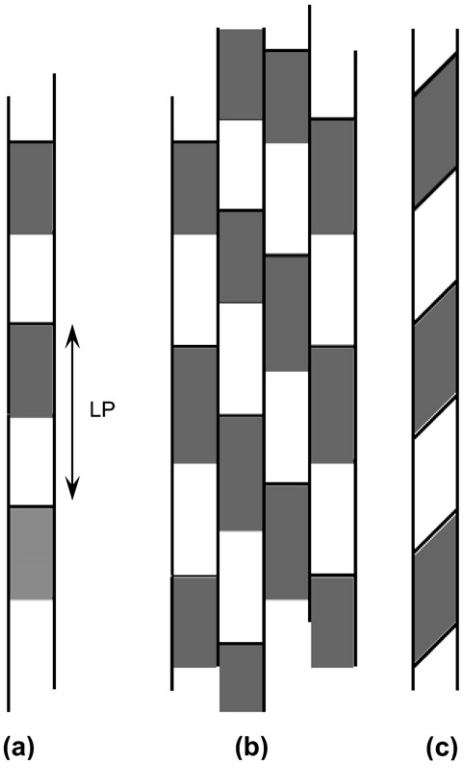

Fig. 8. (a) Schematic diagram of a polymer fibril in which amorphous (white) and crystalline (grey) regions alternate with a fairly regular long period (LP); (b) and (c) possible arrangements of crystalline and amorphous regions which could give rise to a four point pattern. The lamellar thicknesses in this figure and in Fig. 14 are not drawn to scale and are not to be compared with each other.

4. Discussion

4.1. WAXS

The results so far indicate the presence of an intermediate liquid crystalline phase acting as a precursor to crystallisation.

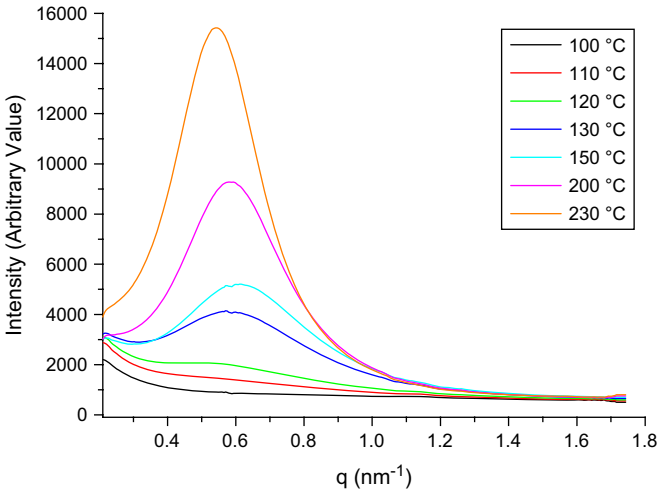

Fig. 9. One-dimensional diffraction profiles of PET, 0.9 IV, obtained by integrating two-dimensional diffraction patterns shown in Fig. 7.

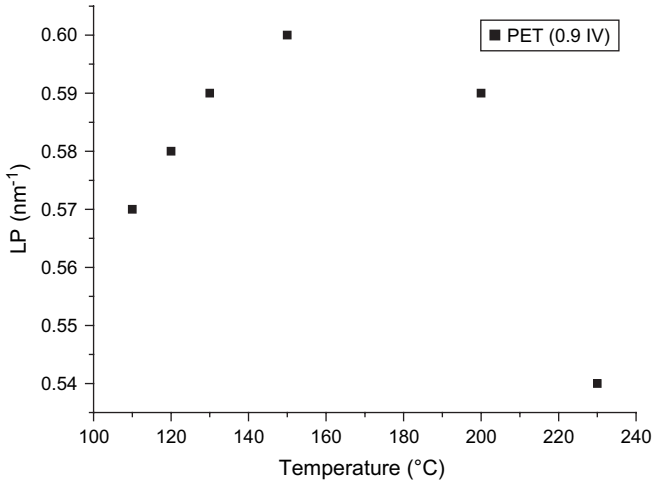

Fig. 10. The change in long period (LP), with increasing temperature for PET (0.9 IV) as obtained from Fig. 9.

The structural arrangement of the mesophase can be described as a smectic-A. We suggest that the step at which the mesophase is formed is the *crystallisation-determining* step that determines the degree of crystallinity at the end of the annealing or the drawing experiment. In fact only these ordered "*segments*" or "*chains*" present in the intermediate smectic-A mesophase are those responsible for forming the crystals.

The amount of the mesophase formed also determines the degree of orientation in the material. During crystallisation the amount of the mesophase degrades, transforming into crystals without it losing its orientation. This transformation helps to relieve the stress exerted on the amorphous regions by inducing tilt in PET [6]. This transformation also causes the reduction of the amount of the oriented component (mesophase) rather than the fall in the degree of orientation of the component [11]. These results come in good agreements with experiments done on PET during drawing [31–33].

4.2. SAXS

Firstly, it is quite obvious that except for the fibre streaking there is no feature that can be observed in SAXS patterns that signifies the appearance of the mesophase as detected by the WAXS discussed above. The fibre streaking has also been observed earlier in PET fibres [34,35]. Secondly, only after crystallisation starts and at temperatures greater than or equal to T_g of the polymer a significant four point pattern can be detected. Thirdly, by increasing temperature this four point pattern changes to a two bar pattern and then to a two point pattern.

This change in the SAXS pattern can be explained according to Rule et al. [26] and Rober et al. [36]. A schematic representation of what might be going on during the process of crystallisation is shown in Fig. 14. This suggests that no SAXS pattern is observed prior to crystallisation i.e. only when crystallites start to appear and are big enough to cause

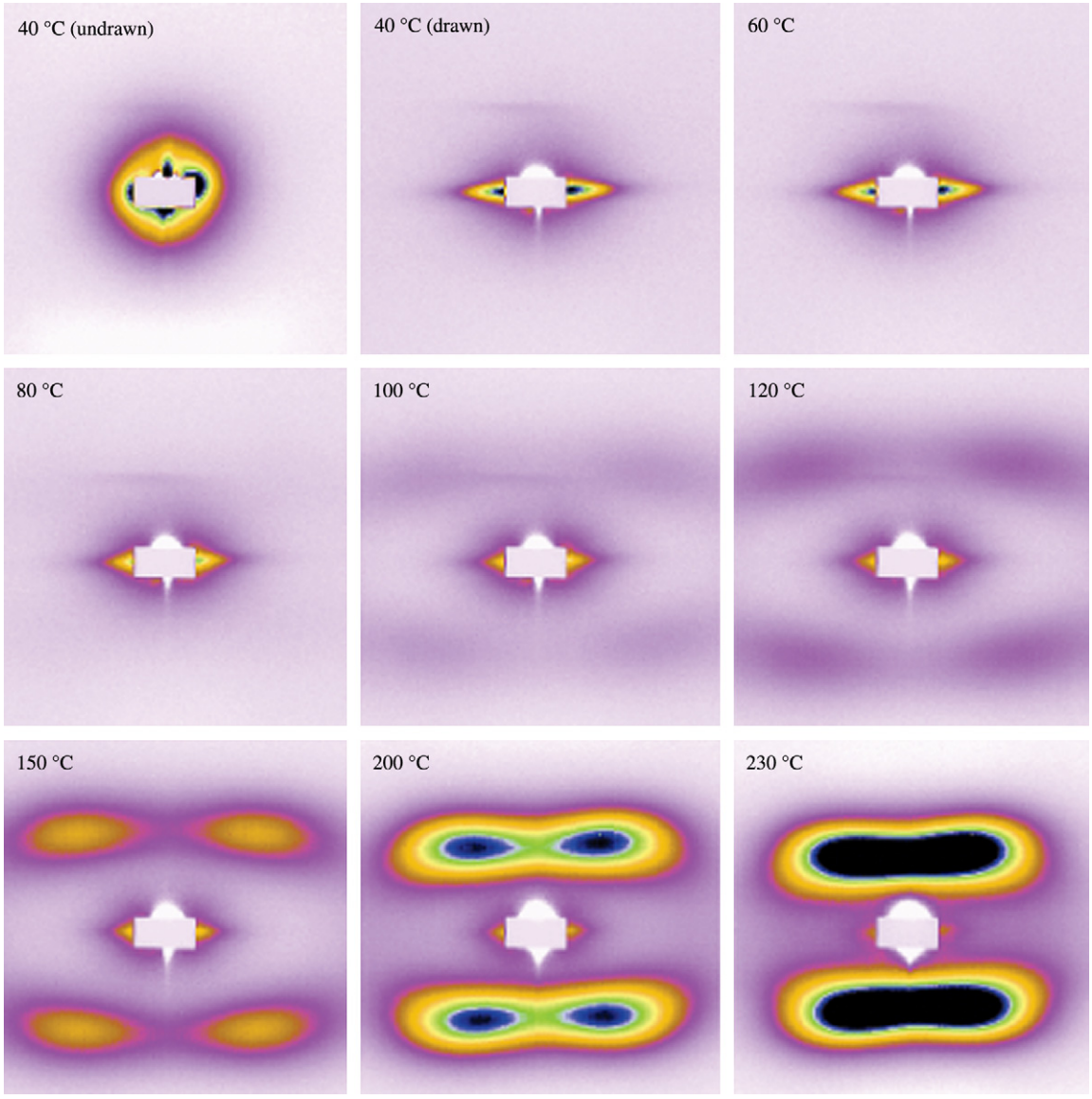

Fig. 11. Two-dimensional diffraction patterns of PET, 0.9 IV, taken at different temperatures as indicated in the figure. The sample has been drawn at 40 °C to a draw ratio of approximately 3.5 and then heated gradually till 230 °C. The first diffraction pattern is taken at 40 °C for an undrawn sample and the second one taken at the same temperature for a drawn sample.

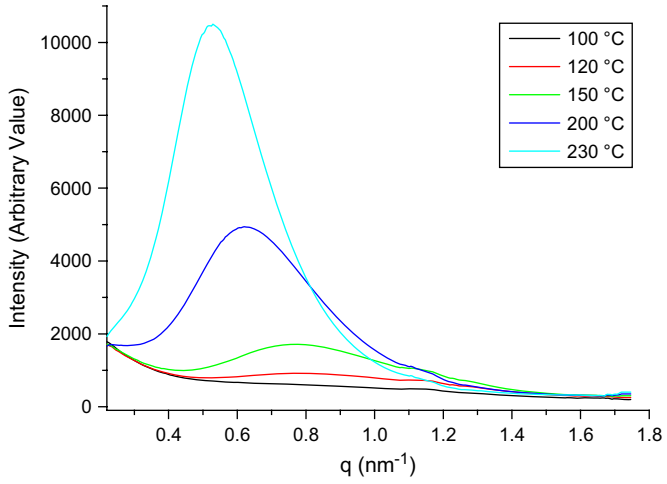

Fig. 12. One-dimensional diffraction profiles of PET, 0.9 IV, obtained by integrating two-dimensional diffraction patterns shown in Fig. 11.

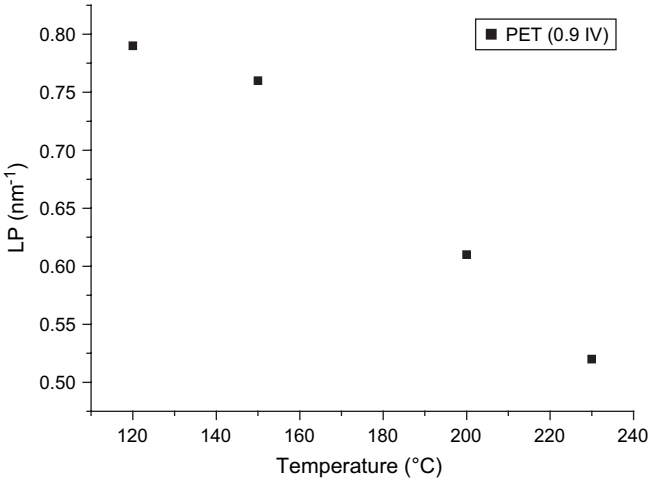

Fig. 13. The change in long period (LP), with increasing temperature for PET (0.9 IV) as obtained from Fig. 12.

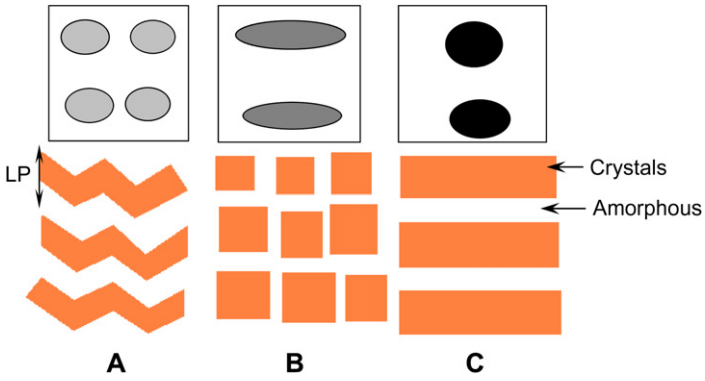

Fig. 14. A schematic representation of the transition between a four point pattern (A) to a two bar pattern (B) to a two point pattern (C) together with the changes in the typical orientation of the polymer structures. The lamellar thicknesses in this figure and in Fig. 8 are not drawn to scale and are not to be compared with each other.

an electron density change detectable by SAXS. During heating the crystals might tend to align readily in the direction of the draw leading to the transformation from a four point SAXS pattern to a two bar one. Further increase in temperature would lead to the merging of the crystallites to form large aggregates as shown in Fig. 14C and the two bar SAXS pattern is transformed into a two point one. The increase in size and the merging of the crystallites together increases the intensity of the observed small angle diffraction pattern. A similar correlation between WAXS and SAXS diffraction patterns has also been discussed on PET samples during drawing [37–39].

5. Conclusions

The results obtained herein indicate that there is a uniform global change taking place over the entire sample during the transition between the oriented amorphous and the oriented crystalline states. The WAXS results discussed here indicate the presence of an intermediate liquid crystalline phase prior to crystallisation. The mesophase is classified as having a smectic-A type order. We also suggest that the formation of the mesophase is the crystallisation determining step based on the results presented in this paper. This suggestion is also supported by the behaviour of 50% PET/PEN random copolymer and presented elsewhere [40]. These results show that the unoriented polymer, where the ordered smectic-A mesophase is not existent, does not crystallise at all upon annealing. It is suggested that a specific experiment is to be designed to monitor the actual fraction of the sample that is transforming to the mesophase and then to the triclinic crystals.

The WAXS experiment did not immediately provide direct evidence of global microstructural changes taking place during annealing in order to determine the microstructural consequences of the formation of the mesophase. However, the SAXS from the mesophase while suggesting the presence of fibrillar arrangement of polymer chains in the direction of the draw, represented by the initial fibre streaking, gives no evidence of density variation which would indicate the presence of any significant microstructure. On the other hand once crystallisation commences on annealing above the glass transition temperature, the SAXS shows very clear evidence of the microstructure, which then develops.

References

[1] Von Bonart R. Kolliod-Zeitschrift und Zeitschrift fur Polymere 1966; 1:213.
[2] Von Bonart R. Kolliod-Zeitschrift und Zeitschrift fur Polymere 1968; 16:231.
[3] Keller A. In: Dosier M, editor. Crystallization of polymers. NATO Advanced Research Workshop. Mons, Belgium: Kluwer; 1992. p. 1.
[4] Imai M, Kaji K, Kanaya T. Macromolecules 1994;27:7103.
[5] Welsh GE, Blundell DJ, Windle AH. Macromolecules 1998;31:7562.
[6] Welsh GE, Blundell DJ, Windle AH. Journal of Materials Science 2000;35:5225.
[7] Asano T, Seto T. Polymer Journal 1973;5:72.
[8] Asano T, Balta Calleja FJ, Flores A, Tanigaki M, Mina MF, Sawatari C, et al. Polymer 1999;40:6475.
[9] Mahendrasingam A, Martin C, Fuller W, Blundell DJ, Oldman RJ, MacKerron DH, et al. Polymer 2000;41:1217.
[10] Mahendrasingam A, Martin C, Fuller W, Blundell DJ, Oldman RJ, Harvie JL, et al. Polymer 1999;40:5553.
[11] Blundell DJ, Mahendrasingam A, Martin C, Fuller W. Journal of Materials Science 2000;35:5057.
[12] Jackeways R, Klien JL, Ward IM. Journal of Materials Science 1996; 37:3761.
[13] Carr PL, Nicholson TM, Ward IM. Polymers for Advanced Technologies 1997;8:592.
[14] Auriemma F, Corradini P, De Rosa C, Guerra G, Petraccone V, Bianchi R, et al. Macromolecules 1992;25:2490.
[15] Auriemma F, Guerra G, Parravicini L, Peraccone V, Russo G. Journal of Polymer Science Part B: Polymer Physics 1995;33:1917.
[16] Nicholson TM, Davies GR, Ward IM. Polymer 1994;35:4259.
[17] Vanderdonckt C, Krumova M, Balta Calleja FJ, Zachmann HG, Fakirov S. Colloid and Polymer Science 1998;276:138.
[18] Berkowitz S. Journal of Applied Polymer Science 1984;29:4353.
[19] Mahendrasingam A, Fuller W, Forsyth VT, Oldman RJ, MacKerron DH, Blundell DJ. Reviews of Scientific Instruments 1992;63:1087.
[20] Middleton AC, Duckett RA, Ward IM, Mahendrasingam A, Martin C. Journal of Applied Polymer Science 2001;79:1825.
[21] Lovell R, Mitchell GR. Acta Crystallographica 1981;A37:135.
[22] Blundell DJ. Polymer 1982;23:359.
[23] Sferrazza M, Crawshaw J, Donald AM, Narayanan T. Macromolecules 2001;34:6708.
[24] Crawshaw J, Sferrazza M, Donald AM. Plastics Rubber and Composites Processing and Applications 2001;30(2):68.

[25] Kadudo M, Kasai N, editors. X-ray diffraction by polymers. Elsevier; 1972. p. 404.
[26] Rule RJ, MacKerron DH, Mahendrasingam A, Martin C, Nye TM. Macromolecules 1995;28:8517.
[27] Alexander LE, editor. X-ray diffraction methods in polymer science. Chichster: Wiley; 1969.
[28] Klug HP, Alexander LE, editors. X-ray diffraction procedures. 2nd ed. John Wiley & Sons Inc; 1974.
[29] Fu Y, Busing WR, Jin Y, Affholter K, Wunderlich B. Macromolecular Chemistry and Physics 1994;195:803.
[30] Fu Y, Annis B, Boller A, Jin Y, Wunderlich B. Journal of Polymer Science Part B: Polymer Physics 1994;32:2289.
[31] Ran S, Wang Z, Burger C, Chu B, Hsiao BS. Macromolecules 2002;35:10102.
[32] Kawakami D, Ran S, Burger C, Fu B, Sics I, Chu B, et al. Macromolecules 2003;36:9275.
[33] Kawakami D, Hsiao BS, Ran S, Burger C, Fu B, Sics I, et al. Polymer 2004;45:905.
[34] Rober S, Bosecke P, Zachmann HG. Makromolecular Chemistry, Macromolecular Symposium 1988;15:295.
[35] Hristov HA, Schultz JM. Journal of Polymer Science Part B: Polymer Physics 1990;28:1647.
[36] Chang H, Lee KG, Schultz JM. Journal of Macromolecular Science: Physics 1994;B33(1):105.
[37] Kawakami D, Hsiao BS, Burger C, Ran S, Avila-Orta C, Sics I, et al. Macromolecules 2005;38:91.
[38] Kawakami D, Ran S, Burger C, Avila-Orta C, Sics I, Chu B, et al. Macromolecules 2006;39:2909.
[39] Uchiyama T, Suyama M, Alam MM, Asano T, Henning S, Flores A, et al. Polymer 2007;48:542.
[40] Abou-Kandil AI, Windle AH, et al. Polymer 2007;48:4824.